STUDIES ON THE EFFECTS OF LAMINA THICKNESS AND ORIENTATION ON THE SHEAR RESPONSE OF COMPOSITE LAMINATES

Haibao Liu [1], Brian G. Falzon [1]*, Giuseppe Catalanotti [1]

[1]School of Mechanical and Aerospace Engineering, Queen's University Belfast, UK, BT9 5AH
Email: hliu07@qub.ac.uk, Web Page: http://www.qub.ac.uk
Email: b.falzon@qub.ac.uk, Web Page: http://www.qub.ac.uk
Email: g.catalanotti@qub.ac.uk, Web Page: http://www.qub.ac.uk

Keywords: Composite materials, Nonlinear shear, Material characterisation, Damage mechanism

ABSTRACT

With the growing application of carbon-fibre reinforced polymers (CFRPs) in lightweight aerospace and transportation structures, it is essential and urgent to develop a comprehensive understanding of their response under various loading conditions to determine the design constraints. Under longitudinal tensile and compressive loading, the material behaviour is dominated by the fibre and presents a predominantly linear response. In contrast, transverse and shear loading may result in large nonlinear deformation prior to polymer matrix damage. Compared to fibre dominated behaviour, a response dominated by the matrix under shear loading can considerably limit the load-bearing capability and restrict the utilisation of composite materials. In the design of composite structures, lamina thickness and orientation are specified to meet the requirements of the working environment. In order to attain a detailed comprehension of the shear response of these parameters, an investigation into the effects of lamina thickness and orientation on the shear response of composite laminates was carried out in this work. Different ply thickness and ply orientation were represented by four composite lay-ups to characterise the material response of composite laminates under shear loading. The geometry of a V-notched rail shear specimen and testing method, presented in the American Society for Testing and Materials (ASTM) standard D7078/D7078M-05, was employed to perform the physical compact shear tests. A Digital Image Correlation (DIC) system was used to observe the strain evolution of the compact shear specimens. The load versus displacement and nominal stress versus strain curves were obtained from the experimental data. In addition, the nonlinear shear stress profile was defined using an exponential model based on the calculated nominal stress and measured strain. The shear modulus, shear strength and nonlinear shear response obtained from different composite lay-ups were compared. A good understanding of the relationship between shear response and lay-up thickness and orientation was achieved based on experimental and analytical results obtained in this study. Furthermore, the measured shear properties of the composite laminates were used to verify a high-fidelity computational damage model through the modelling of virtual v-notched rail tests. Good correlation was obtained between experiment and simulation results.

1 INTRODUCTION

Utilisation of composite materials in advanced light weight structures has brought considerable benefits to the aviation industry [1,2]. Composite structures which have high strength-to-weight and high stiffness-to-weight ratios have made a big contribution to reduce operational cost. Accurate measurement of composite material properties is required for the better design and optimisation of composite structures. Among all the design properties that need to be measured, in-plane shear modulus, strength and ultimate strain are important design parameters. Generally, unidirectional (UD) composite laminates present excellent mechanical properties under longitudinal loading, where the response of materials is dominated by carbon-fibres. In contrast, large nonlinear deformation and subsequent matrix cracking, i.e., matrix-dominated failure might be induced under transverse or shear loading in composite structures. As a key design factor, the shear response including in-plane shear

modulus, strength and ultimate strain are important design parameters which need to be accurately measured [3–5].

Many experimental methods are available for evaluating the shear properties of coupons such as the rail shear test [6], short beam tests [7], $\pm 45^{\circ}$ tensile shear test [8]and V-notch beam test [9]. One of the main difficulties in measuring the shear properties of these materials is in generating a pure shear stress state in the gauge section of a test specimen. The V-Notched Rail shear test method (ASTM standard D7078/D7078M_12) [9] is essentially a combination of the best features of two commonly used methods, the Iosipescu Shear [10] and the rail shear test methods [6], generating a relatively uniform shear stress state within a larger gauge section between V-notches.

In addition, the demand for a reliable predictive model is another impetus to investigate the material properties of composite laminates. High-capability numerical tools are able to reduce the extent of physical testing during the development of composite structures. Furthermore, such tools give the possibility of predicting further insight into complex damage mechanisms, enabling better exploitation of these materials in composite structures. In order to achieve the capability in predicting the material response of composites, the accurate measurement of material properties, especially the associated nonlinearities, is a necessary and important step in the development of a robust model [11–13].

Considerable efforts have been expended in investigating the shear response of composite laminates. Almeida Jr. et al. [14] used four testing methods to capture the shear response of glass-fibre reinforced composites. Five composite lay-ups, $[0]_5$, $[90]_5$, [0/90/0/90/0] and randomly oriented (mat), were employed to investigate the effects of the lay-up configurations on in-plane shear properties of glass fibre reinforced epoxy composites. In these five lay-ups, the randomly oriented lay-up presented higher in-plane shear strength due to its random fibre orientation. The dynamic shear modulus was higher for the $[0]_5$ lay-up as expected due to the longitudinally oriented fibres. The V-notched rail shear test described in ASTM Standard D 7078 was adopted by Akats et al. [5] to investigate the effects of the material orientation and notch angle of V-notched rail shear specimens on in-plane shear properties. A modified Iosipescu test fixture was designed and manufactured by Khashaba [15] to investigate the in-plane shear properties of cross-ply composite laminates with different off-axis angles. The laminates were cut at different off-axis angles to give specimens with different stacking sequences. The maximum in-plane shear strength was found for specimens with 45° and 60° off-axis angles, and specimens with 0° and 90° off-axis angles presented the minimum in-plane shear strength in all tested specimens. Based on accurate material characterisation, Tan and Falzon [16] developed a high-fidelity numerical model to capture the nonlinear shear response of carbon-fibre reinforced composite laminates. The model was shown to accurately predict the constitutive response in terms of permanent plastic strain, degraded modulus as well as load reversal. The development of this physically-based damage model which has a reliable predictive capability fully highlighted the importance of the accurate measurement of composite nonlinear properties.

In this work, an investigation on the effects of lamina thickness and orientation on the shear response of composite laminates was carried out. Different ply thickness and ply orientation were represented by four composite lay-ups to characterise the material response of composite laminates under shear loading. The V-notched rail shear testing method presented in ASTM Standard D 7078 was used to implement the physical tests. A Digital Image Correlation (DIC) system was employed to detect the strain evolution of the V-notched shear specimens[17]. The material properties including laminate shear modulus, first-ply failure shear strength, hardening strength and nonlinearity were obtained from the experimental data. Material properties attained from different composite lay-ups were compared to discuss the influence of lamina thickness and orientation on the composite shear response. A good understanding of the shear response of composite laminates was achieved based on experimental and analytical results. Furthermore, corresponding virtual v-notched rail shear tests were carried out using a verification model with the characterised shear properties. The simulation results correlated well with experimental results.

2 MATERIALS AND METHODS

The composite material system used in this work is HMC/SL84LV unidirectional carbon-fibre/epoxy composite pre-preg. The specimens were manufactured using hand lay-up. The preformed laminated composites were cured in a vacuum environment. To ensure the quality of the specimens, all panels were subsequently inspected using a Non-Destructive Inspection (NDI) system (Figure 1) to make sure the pristine specimens were free of any major defect.

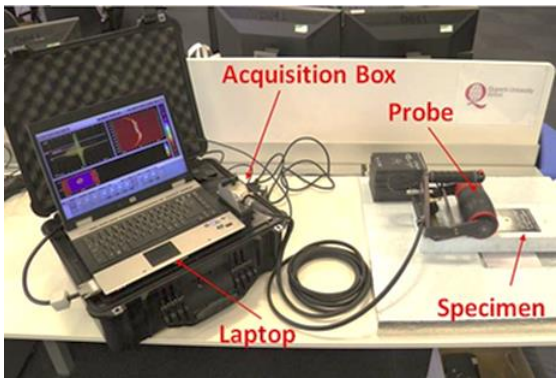

Figure 1: Non-destructive inspection system.

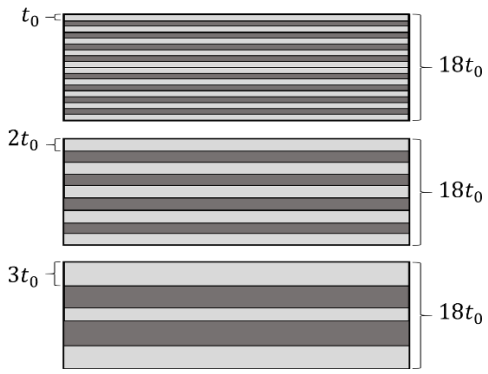

Figure 2: Sketch of sample cross section (t_0 equals reference ply thickness).

The mechanical properties of a single composite ply were measured using standard test methods and these are given in Table 1.

Properties	Modulus (GPa)	Poisson`s ratio	Strength (MPa)
Value	$E_{11} = 198;$ $E_{22} = E_{33} = 6.39;$ $G_{12} = G_{13} = 4.31;$ $G_{23} = 2.39;$	$\nu_{12} = \nu_{23} = \nu_{13} = 0.337;$	$X^T = 1562;\ X^C = 843;$ $Y^T = 28.8;\ Y^C = 83.1;$ $S_{12} = 64.7$

Table 1: Mechanical properties of HMC/SL84LV pre-preg.

The specimen configuration presented in ASTM D70781/D7078M-05 was adopted in this work. A band saw and a milling cutter were used to machine the profile of the specimen and introduce the V-notch, respectively. Specimens with same laminate thickness but different ply thickness were designed as shown in Figure 2, where t_0 is the datum thickness which equals the single ply thickness of V-notched Rail Shear Standard (VRS-S) samples. The dimensions of the specimen are shown in Figure 3 and Table 2, where VRS-B represents the V-notched Rail Shear Blocked samples, VRS-D represents the V-notched Rail Shear Double-blocked samples, and VRS-Q represents the V-notched Rail Shear Quasi-isotropic samples.

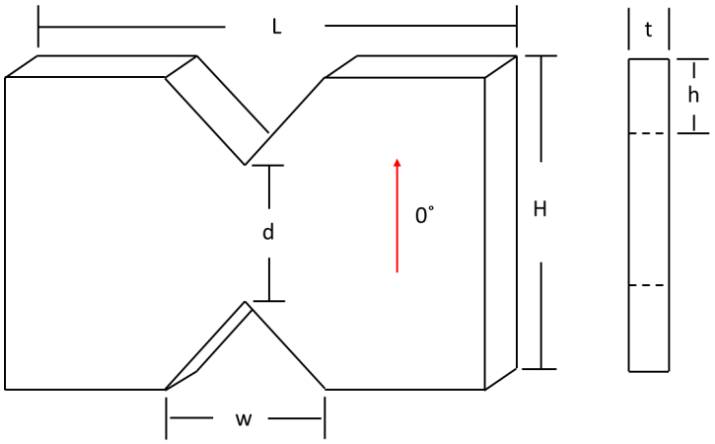

Figure 3: Dimensions of v-notched rail shear specimen (all dimensions are in mm).

Specimen code	Lay-ups	Number of samples	L	H	t	d	w	h
VRS-S	$[(0/90)_4/0]_S$	3	76	56	5.2	31	25	12.5
VRS-B	$[(0_2/90_2)_2/0]_S$	3	76	56	5.2	31	25	12.5
VRS-D	$[(0_4/90_4)/0]_S$	3	76	56	5.2	31	25	12.5
VRS-Q	$[(0/+45/90/-45)_2/0]_S$	3	76	56	5.2	31	25	12.5

Table 2: Geometries and lay-ups of v-notched rail shear specimens (all dimensions are in mm).

3 EXPERIMENT AND EQUIPMENT

The V-notched Rail Shear (VRS) tests were carried out on a Hounsfield screw-driven testing machine which has a 50kN load cell. During the test, displacement control was applied at a crosshead displacement of 1mm/min. A Digital Correlation System (DIC) was set up at front of the testing machine to monitor the strain evolution of the VRS specimens, and the tracking intervals of the DIC system was set as 0.2ms. The VRS specimen was speckled using white paints and clamped by a rigid rail-shear fixture during the test. The experimental set-up and fixtures for v-notched rail shear tests are shown in Figure 4 and Figure 5, respectively.

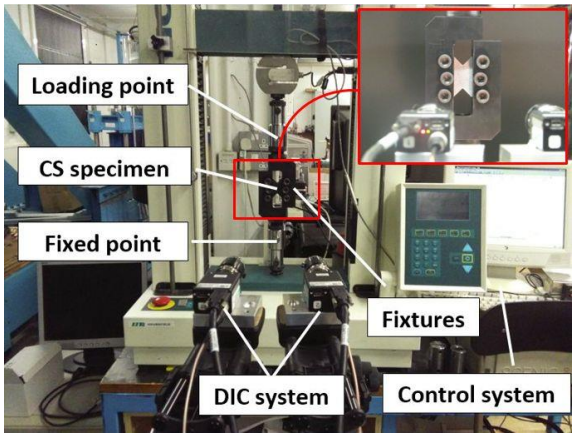

Figure 4: Experimental apparatus for VRS tests.

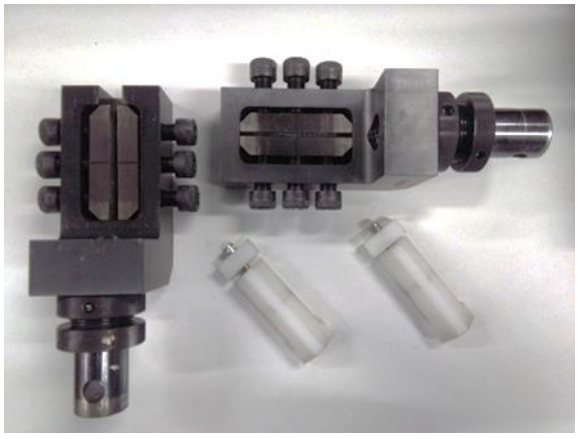

Figure 5: Fixtures for VRS tests.

4 DATA REDUCTION

In this work, the scheme described in ASTM D7078 was used to carry out the data reduction. The nominal shear strength, S, was calculated as

$$S = \frac{P_{max}}{A} \tag{1}$$

where, P_{max} is the maximum load and A is the area of the cross-section along the ligament, which is calculated by the distance between two notch tips, d, and the thickness t. The equation is given as

$$A = d \times t \tag{2}$$

The MATLAB R2016a was used to yield fitting curves which best fits the stress-strain data points obtained from V-notched rail shear test. Exponential function as shown in Eq. (3) is applicable to the curve fitting.

$$(\gamma_{ij}) = c_1\left[exp(c_2\gamma_{ij}) - exp(c_3\gamma_{ij})\right] \tag{3}$$

5 RESULTS AND DISCUSSION

5.1 Effects of lamina thickness

Figure 6a shows the load-displacement curves obtained from VRS specimens with different ply thicknesses. The load versus displacement curves of composite laminates under shear loading contain two main stages: the first stage is the matrix-dominated stage (nonlinear process), and the second is the fibre dominated stage (hardening process). The turning point between two stages is the first ply failure point. The load corresponding to first ply failure was named as first ply failure load, which is also the maximum load in matrix-dominated stage. Before reaching the first ply failure point, tested samples presented nonlinear shear response, which is shown in the stress-strain fitting curves (Figure 6b) obtained from VRS samples using DIC system. As shown in the figure, composite laminates with larger ply thickness exhibited lower laminate shear modulus. The definition of these fitting curves for describing the nonlinear shear response of tested VRS samples is shown in Table 3. Samples with different ply thicknesses started to present different response from first ply failure (FPF) point. Figure 7a exhibits relationship between the first-layer-failure (FPF) strength and ply-thickness. As shown in this figure, the samples with the thinner ply thickness presented higher FPF strength compare to thicker ply-thickness samples (VRS-S > VRS-B > VRS-D). After the first ply failure point, the load of VRS-S samples continued to increase, while, VRS-B and VRS-D samples showed different degrees of decline in load. The following process is the hardening process which is dominated by fibres. The maximum load in this fibre-dominated stage was named as "laminate shear strength". The nominal laminate shear strength can be calculated using Eq. (1). The comparison of nominal laminate strengths obtained from VRS samples is shown in figure 7b.

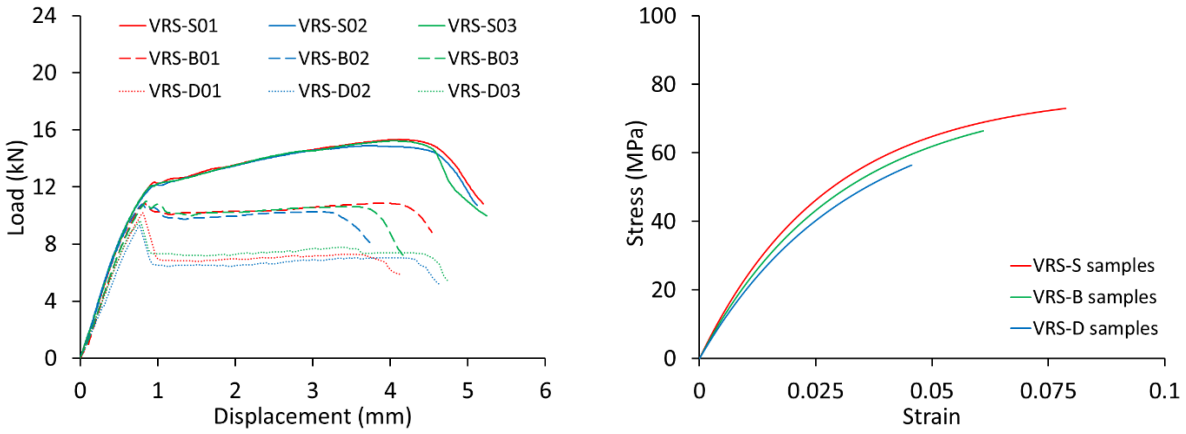

(a) (b)

Figure 6: (a) Load versus displacement curves and (b) stress-strain fitting curves for nonlinear process obtained from v-notched shear tests.

Specimen code	Lay-ups	c_1	c_2	c_3
VRS-S	$[(0/90)_4/0]_S$	76.5	0.12	-36.8
VRS-B	$[(0_2/90_2)_2/0]_S$	71.5	0.73	-35.3
VRS-D	$[(0_4/90_4)/0]_S$	65.9	1.42	-34.2

Table 3: Geometries and lay-ups of V-Notched rail shear specimens.

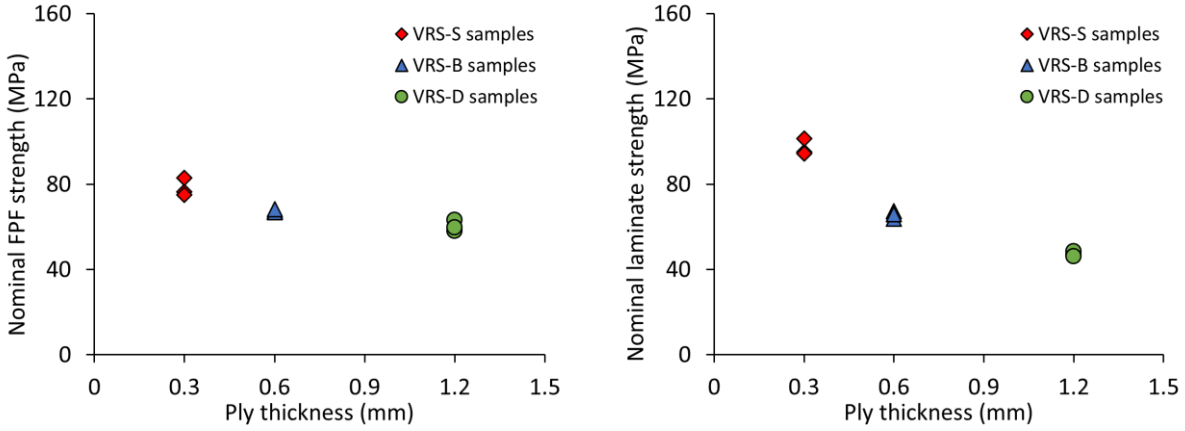

(a) (b)

Figure 7: (a) First ply failure (FPF) strength versus ply thickness and (b) hardening strength versus ply thickness obtained from VRS samples.

5.2 Effects of lamina orientation

As shown in Table 3, VRS-S samples and VRS-Q samples have the number of layers. The difference is VRS-Q samples contain some $\pm 45°$ plies. The results obtained from VRS-S samples and VRS-Q samples were compared to observe the effects of lamina orientation on the shear response of laminated composites. The load-displacement curves are shown in Figure 8a. In this figure, VRS-Q samples presented very high shear stiffness and almost elastic response before the first ply failure point. As shown in Figure 8b, VRS-Q samples also extracted much higher first-layer-failure strength and laminate shear strength than VRS-S samples. In the shear tests, the $\pm 45°$ plies in VRS-Q samples were mainly under tensile loading rather than shear loading, as a result, the load required to facture the $\pm 45°$ plies in these samples should be equivalent or larger than the lamina tensile strength which is much larger than the shear strength. In this way, $\pm 45°$ plies make a big contribution towards increasing the shear bearing capability of composite laminates.

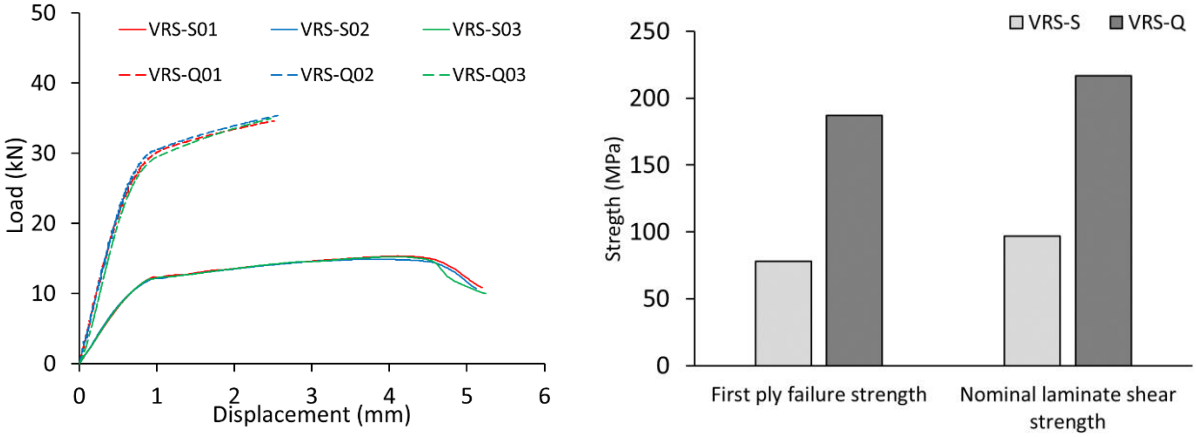

(a) (b)

Figure 8: (a) First ply failure (FPF) strength versus ply thickness and (b) hardening strength versus ply thickness obtained from VRS samples.

5.3 Damage investigation

The initial strain state and final strain state are shown in Figures 9a and 9b respectively. In the finial strain state, obvious strain concentration was observed in the ligament area. This is also correlated with the final fracture surface obtained from tested VRS specimens. An example of a failed VRS specimen is show in Figure 9b, where a clear crack through the ligament can be observed. As shown in Figures 10a-d, fracture surfaces alone the ligament were obtained from different types of VRS specimens. Fibres initially perpendicular to the loading direction presented different degrees of rotation. Rotated fibre bundles can be clearly observed on the fracture surface of VRS-S samples. In the VRS-Q samples, ±45° plies did not show apparent rotation, which means the ±45° plies were under tensile loading rather than shear loading.

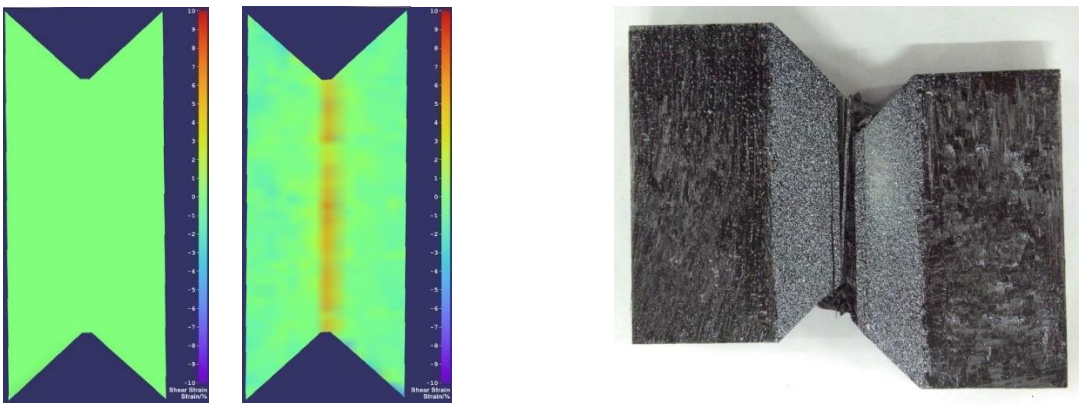

(a) (b)

Figure 9: (a) Initial and final strain distribution captured by DIC system, (b) an example of failed V-notched rail shear specimen.

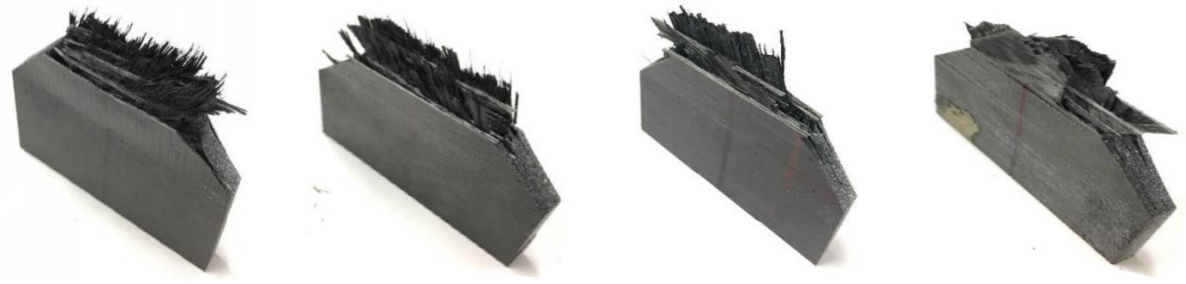

(a) (b) (c) (d)

Figure 10: Fracture surfaces obtained from (a) VRS-S (b) VRS-B (c) VRS-D and (d) VRS-Q samples.

6 NUMERICAL SIMULATION

In order to capture the nonlinear behaviour of composite laminates, a damage model with an in-house VUMAT subroutine was developed in Abaqus/explicit. The FE model was built up according to the set-up shown in Figure 11. In this model, $1mm \times 1mm \times single\ ply\ thickness$ C3D8R elements were employed in the central area. General contact algorithm and friction coefficient of 0.3 was used in the global contact. In-built cohesive surface function was adopted to define the interface interaction of composite laminates.

In this work, the nonlinear shear responses of different composite lay-ups were measured using the combination of tensile testing machine and DIC system. Afterwards, these nonlinear behaviours were described using a series of exponential fitting curves which were defined by corresponding coefficients as shown in Table 3. These coefficients were input into the developed damage model for capturing the shear response of composite laminates. This damage model was verified by simulating the corresponding V-notched rail shear test. As shown in the Figure 12, VRS-S samples were selected as an example to show the typical failure in virtual VRS test. A clear fracture band was observed alone the ligament of the VRS-S sample.

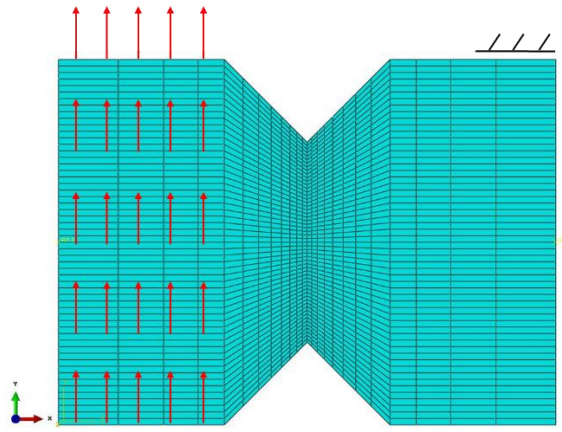

Figure 11: Finite element model

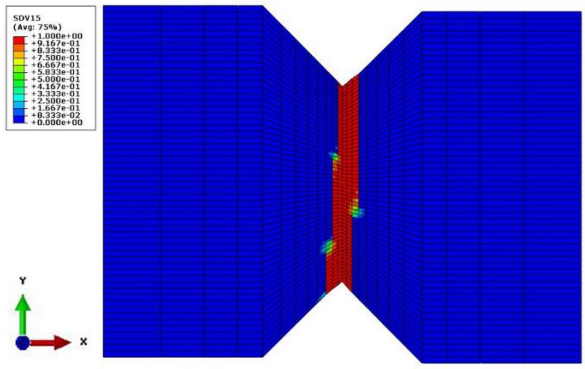

Figure 12: Damaged virtual VRS-S sample

The simulation results obtained from VRS-S, VRS-B and VRS-D samples were compared with corresponding experimental results. As shown in Figures 13a-c, good correlation was achieved between physical tests and numerical simulation. The nonlinear shear response presented by composite laminates with different ply thickness was reproduced by the damage model which contains the physically-based nonlinearity material model.

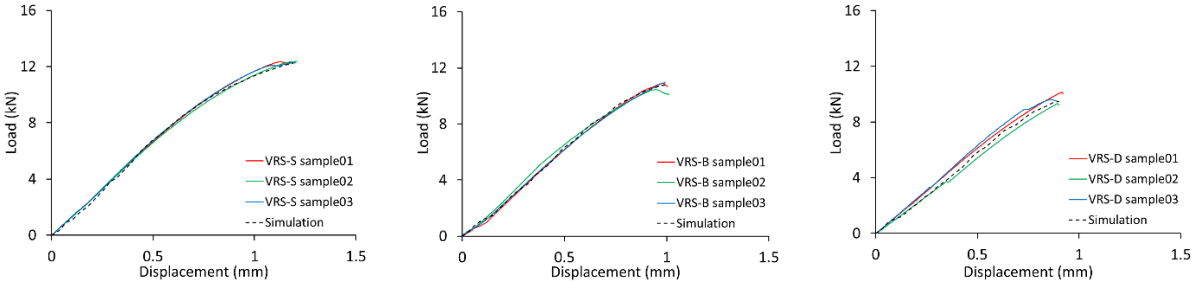

(a) (b) (c)

Figure 13: Damaged virtual VRS-S sample

7 CONCLUSIONS

The shear response of composite laminates plays an important role in the design of composite structures. In this work, four composite lay-ups were designed and tested based on the ASTM standard D7078/D7078M-05 to discuss the effects of ply thickness and orientation on the shear response of composite laminates. All composite lay-ups used in this study have the same overall thickness of 5.2mm. The experiment results showed the VRS-S specimen that was made of thinner plies presented higher shear strength than the VRS-B and VRS-D specimens with blocked (thicker) plies. Based on the damage investigation, it was found that VRS-D specimen exhibited more delamination and debonding damage, which reduced the shear strength significantly, than VRS-S and VRS-B samples. The VRS-Q specimen that has some 45° plies delivered the highest shear strength among these three composite lay-ups. This phenomenon can be explained as most of the shear loading was converted to tensile loading on the ±45° lamina. The nonlinear shear profiles for different composite lay-ups were obtained according to the experimental data, and the influence of the lay-ups on the nonlinearity of composites was discussed. Defined nonlinear shear profiles were entered into the developed damage model for reproducing the shear response of composite laminates. The simulation results correlated well with corresponding experimental results.

ACKNOWLEDGEMENTS

The corresponding author acknowledges the financial support provided by Bombardier and the Royal Academy of Engineering. The authors would like to acknowledge Mr Denis Dalli and Mr Gareth Chisholm from Queen`s University Belfast for their assistance with the experimental phase of this work.

REFERENCES

[1] Masaharu Iwamotoa, Qing-Qing Nib, Teruhiko Fujiwarac and Ken Kurashikib. Intralaminar fracture mechanism in unidirectional CFRP composites. *Engineering Fracture Mechanics*, 64: 721–45, 1999.

[2] Wei Tan, Brian G. Falzon, Mark Price and Haibao Liu. The role of material characterisation in the crush modelling of thermoplastic composite structures. *Composite Structures*, 153: 914–27, 2016.

[3] R. K. Joki, F. Grytten, B. Hayman. Nonlinear response in glass fibre non-crimp fabric reinforced vinylester composites. *Composites Part B: Engineering*, 77: 105–11, 2015.

[4] Robert Brett Williams. Nonlinear Mechanical and Actuation Characterization of Piezoceramic Fiber Composites. PhD thesis, Virginia Polytechnic Institute and State University, 2004.

[5] Mehmet AKTAS, Mehmet Emin DENIZ. Determination of In-Plane Shear Properties of Composite Laminates. *Electronic Journal of Machine Technologies*, 7: 13–23, 2010.

[6] American Society for Testing and Materials. ASTM D4255 / D4255M - 01, Standard Test Method for In-Plane Shear Properties of Polymer Matrix Composite Materials by the Rail Shear Method. *West Conshohocken*, PA, 2001.

[7] American Society for Testing and Materials. ASTM D2344 / D2344M - 16, standard test

method for short-beam strength of polymer matrix composite materials and their laminates. *West Conshohocken*, PA, 2000.

[8] American Society for Testing and Materials. ASTM D3518/D3518M – 94, standard test method for in-plane shear response of polymer matrix composite materials by tensile test of a ±45 laminate. *West Conshohocken*, PA, 2000.

[9] American Society for Testing and Materials. ASTM D7078/D7078M —05, standard Test Method for Shear Properties of Composite Materials by V-Notched Rail Shear Method. *West Conshohocken*, , 2005.

[10] American Society for Testing and Materials. ASTM D5379 / D5379M - 12, standard Test Method for Shear Properties of Composite Materials by the V-notched Beam Method. *West Conshohocken*, PA, 2012.

[11] Travis A. Bogetti, Christopher P.R. Hoppel, Vasyl M. Harik, James F. Newill and Bruce P. Burns. Predicting the nonlinear response and progressive failure of composite laminates. *Composites Science and Technology*, 64: 329–42, 2004.

[12] M. Vogler, R. Rolfes and P.P. Camanho. Modeling the inelastic deformation and fracture of polymer composites - Part II: Smeared crack model. *Mechanics of Materials*, 59: 36–49, 2013.

[13] D. Fanteriaa and E. Panettieria. A non-linear model for in-plane shear damage and failure of composite laminates. *Aerotecnica Missili & Spazio*, 93: 17–24, 2014.

[14] Jos éHumberto S. Almeida Jr. , Clarissa C. Angrizani, Edson C. Botelho and Sandro C. Amico. Effect of fiber orientation on the shear behavior of glass fiber/epoxy composites. *Materials & Design*, 65: 789–95, 2015.

[15] U.A. Khashaba. In-plane shear properties of cross-ply composite laminates with different off-axis angles. *Composite Structures*, 65: 167–77, 2004.

[16] Wei Tan and Brian G. Falzon. Modelling the nonlinear behaviour and fracture process of AS4/PEKK thermoplastic composite under shear loading. *Composites Science and Technology*, 126: 60–77, 2016.

[17] G. Catalanotti, P.P. Camanho, J. Xavier, C.G. D ávila, A.T. Marques. Measurement of resistance curves in the longitudinal failure of composites using digital image correlation. *Composites Science and Technology*, 70: 1986–93, 2010.